Advances in Nano Research, *Vol. 12, No. 5 (2022) 489-499*
https://doi.org/10.12989/anr.2022.12.5.489

Differentiation among stability regimes of alumina-water nanofluids using smart classifiers

Bahador Daryayehsalameh[1], Mohamed Arselene Ayari[2,3], Abdelouahed Tounsi[4,5], Amith Khandakar[6] and Behzad Vaferi*[7]

[1]*School of Chemical Engineering, Iran University of Science and Technology (IUST), I.R. Iran*
[2]*Department of Civil and Architectural Engineering, College of Engineering, Qatar University, Doha 2713, Qatar*
[3]*Technology Innovation and Engineering Education Unit, Qatar University, Doha 2713, Qatar*
[4]*YFL (Yonsei Frontier Lab), Yonsei University, Seoul, Korea*
[5]*Material and Hydrology Laboratory, University of Sidi Bel Abbes, Faculty of Technology, Civil Engineering Department, Algeria*
[6]*Department of Electrical Engineering, Qatar University, Doha 2713, Qatar*
[7]*Department of Chemical Engineering, Shiraz Branch, Islamic Azad University, Shiraz, Iran*

(*Received August 10, 2021, Revised February 14, 2022, Accepted March 2, 2022*)

Abstract. Nanofluids have recently triggered a substantial scientific interest as cooling media. However, their stability is challenging for successful engagement in industrial applications. Different factors, including temperature, nanoparticles and base fluids characteristics, pH, ultrasonic power and frequency, agitation time, and surfactant type and concentration, determine the nanofluid stability regime. Indeed, it is often too complicated and even impossible to accurately find the conditions resulting in a stabilized nanofluid. Furthermore, there are no empirical, semi-empirical, and even intelligent scenarios for anticipating the stability of nanofluids. Therefore, this study introduces a straightforward and reliable intelligent classifier for discriminating among the stability regimes of alumina-water nanofluids based on the Zeta potential margins. In this regard, various intelligent classifiers (i.e., deep learning and multilayer perceptron neural network, decision tree, GoogleNet, and multi-output least squares support vector regression) have been designed, and their classification accuracy was compared. This comparison approved that the multilayer perceptron neural network (MLPNN) with the SoftMax activation function trained by the Bayesian regularization algorithm is the best classifier for the considered task. This intelligent classifier accurately detects the stability regimes of more than 90% of 345 different nanofluid samples. The overall classification accuracy and misclassification percent of 90.1% and 9.9% have been achieved by this model. This research is the first try toward anticipting the stability of water-alumin nanofluids from some easily measured independent variables.

Keywords: alumina-water nanofluids; artificial intelligent classifiers; classification accuracy; multilayer perceptron; stability regime

1. Introduction

High-temperature stream/equipment of industrial processes are often required to cool down using an appropriate working/operating fluid (Ebadian and Lin 2011). It is widely accepted that a liquid-based cooling technology can effectively cool down high-temperature equipment (Ebadian and Lin 2011). Deionized water, ethylene glycol, high heat capacity oils, and propane are the most commonly used liquids in cooling cycles (Lai *et al*. 2009). Unfortunately, these traditional cooling media often fail to transfer heat adequately flux due to their weak thermophysical characteristics (Kazemi and Nasr 2014). On the other hand, some devices are needed to cool down as quickly and efficiently as possible by removing a massive heat flux (Ebadian and Lin 2011).

The addition of nano-sized metal and non-metallic particles to the traditional cooling liquids (i.e., nanofluid synthesis) has been proposed to improve their thermo-physical properties and heat removal efficiency (Khalifeh and Vaferi 2019). Nanoparticles Brownian motion (Iqbal *et al*. 2021) and their higher thermal conductivity than the traditional fluids (Ibrahim *et al*. 2021) are responsible for this improvement. Generally, nanofluids are fabricated by homogenized dispersion of single or combined nano-particles in a pure (Pandit and Sharma 2020) or mixture (Asadi *et al*. 2021) of traditional liquid. Nanofluids have already approved their potential advantages to cover the limitations of conventional fluids in heat transfer applications (Abid *et al*. 2020, Sharif *et al*. 2021a, b).

Nano-scale particles (Kaabipour and Hemmati 2021) have been gradually engaged in different applications ranging from wastewater treatment (Keshtkar *et al*. 2021, Alibak *et al*. 2022), nanocomposite fabrication (Arani *et al*. 2021, Esmaeili-Faraj *et al*. 2021, Nezhad *et al*. 2021), tunable polymer-protein (Seaberg *et al*. 2020), antibacterial media (Baláž *et al*. 2019), energy generation (Chu *et al*. 2021) and management (Chu *et al*. 2020a, b, Gul *et al*. 2020, Haq *et al*. 2021), reforming process (Deng *et al*. 2019), porous media (Esfe *et al*. 2020, Sheikholeslami *et al*. 2021), nanofluid synthesis (İpek and Mermerdaş 2020, Khan *et al*. 2021, Ali *et al*. 2021) to trace gold separation

*Corresponding author, Professor,
E-mail: behzad.vaferi@gmail.com

ISSN: 2287-237X (Print), 2287-2388 (Online)

from water (Zeng *et al*. 2021).

Stabilizing the nanoparticles in a base fluid is a limiting/hindering step for nanofluids to achieve their highest potential in industrial and real-life applications (Khalifeh and Vaferi 2019). Nanofluid's transport and thermophysical properties and their potential application as cooling media are directly related to the stability regimes (Mukherjee *et al*. 2018). Synthesizing a homogeneous nanofluid so that the nanoparticle tendency to either aggregate or precipitate be as slight as possible is still a technical challenge (Yang *et al*. 2011, Mahajan 2017). Indeed, nanoparticles' high specific surface area (surface area per mass) creates a strong van der Waals force that adheres them together and forms aggregates (Mukherjee *et al*. 2018). These phenomena increase the nano-aggregate size and unstable nanofluids (Khalifeh and Vaferi 2019). Unstable nanofluids experience nanoparticles' sedimentation, mobility reduction, and deterioration in the transport and thermophysical characteristics (Angayarkanni and Philip 2014). The effects of aggregation on the flow characteristics (Bao *et al*. 2019), thermal conduction (Khalifeh and Vaferi 2019), viscosity (Kole and Dey 2011), optical (Song *et al*. 2016), and transport (Kang *et al*. 2012) properties of nanofluids have comprehensively been investigated.

Surface modification, mechanical or ultrasonic agitation, and pH adjustment are general techniques to fabricate stable nanofluids (Zhou *et al*. 2021, Ghadimi 2013). A single or combination of these techniques may be applied to synthesize a stabilized nanofluid (Khalifeh and Vaferi 2019). Generally, no universal guideline exists to anticipate the best scenario to synthesize a nanofluid with the highest possible stability (Ghadimi 2013). Several attempts have been made to stabilize nano-suspensions using surface-active agents, i.e., surfactants (Ghadimi 2013), acidity adjustment (Cacua *et al*. 2019), ultrasonic agitation (Ghadimi 2013), surface modification (Li *et al*. 2014), and mechanical agitation (Wen *et al*. 2018).

While it is widely accepted that unstable nanofluids are not appropriate cooling media, their stability must be carefully monitored before engaging in real-field applications. Zeta potential is a well-established method for quantitatively determining stability regimes of a nano-suspension (Ghadimi 2013). Since nanofluid stability has a complex dependency on several factors, it often needs high costs and efforts to be determined by experimental inspection. On the other hand, there are no empirical, semi-empirical, and even intelligent scenarios for anticipating the stability regime of nanoparticles dispersion in a base fluid (Ghadimi 2013). Therefore, this study introduces a straightforward intelligent classifier to differentiate among the stability regimes of alumina-water nanofluids based on the zeta potential margins. The most accurate classifier is found by comparing the classification accuracy of deep learning neural network, decision tree, multilayer perceptron neural network, GoogleNet, and multi-output least squares support vector regression. Nanofluid characteristics (temperature, pH, nanoparticle type, and dosage), surfactant type and concentration, and ultra-sonication properties (duration, frequency, and power), are deciding factors to determine the stability regimes. This research can be viewed as the first try towards anticipting the stability of water-alumin nanofluids from some easily measured independent variables.

Table 1 Classification of the nano-suspension stability regimes based on the absolute value of the Zeta potential test (Mukherjee *et al*. 2018)

Zeta potential (absolute value)	Stability/instability regime
Zeta potential = 0 mV	Slight to no stability (**Class 1**)
0 mV < Zeta potential <= 15 mV	Less stability with light settling (**Class 2**)
15 mV < Zeta potential <= 30 mV	Moderate stability (**Class 3**)
30 mV < Zeta potential <= 45 mV	Decent stability with possible settling (**Class 4**)
45 mV < Zeta potential <= 60 mV	Excellent stability with lesser possibility of settling (**Class 5**)

2. Materials and methods

The first part of this section introduces the stability regimes of nano-suspensions based on the Zeta potential margins. The second part presents the collected experimental database used to classify the alumina-water stability regimes.

2.1 Stability of nanofluids

Light scattering, ultraviolet-visible spectrophotometer, photo-capturing, transmission electron microscopy, scanning electron microscope, sedimentation mass balance, and Zeta potential are available methods to monitor the stability regimes of nano-suspensions (Ghadimi 2013). The latter is likely the most reliable test to determine the nanofluid stability regimes. The Zeta potential test investigates the electrophoretic forces between nano-particles in the base fluid. Determination of the suspension stability from the zeta-potential arises from a simple scientific fact that states the similarly charged particles naturally tend to repulse each other. Indeed, the nano-sized particles with low surface charges tend to form an aggregate and unstabilize nano-suspension. In other words, the electrostatic repulsions between nanoparticles and nanofluid stability increase by increasing the absolute value of zeta potential (Mukherjee *et al*. 2018). Table 1 introduces the stability regimes of nano-suspension based on the absolute value of a Zeta potential margin.

2.2 Literature data

A relatively massive experimental database for the stability of alumina-water nanofluids has been collected from 29 different experimental research studies (Table 2). To the best of our knowledge, there are no other data for alumina-water stability regimes in the literature. Our database includes the stability information of 345 water-alumina samples. Table 2 shows that the alumina-water stability regime is considered as a function of nanofluids characteristics (temperature, pH, and alumina concentration in base fluids), ultrasonic agitation properties (power,

Table 2 Summary of literature data about stability regimes of alumina-water nano-suspensions

F1	F2	F3	F4	F5	F5	F7	F8	F9	R1	References
0.030	3	0.553	1.3-13.4	130	60	100	40	298	29.1-40.7	(Huang *et al*. 2009)
0.500	0	0.000	7.0	105-213	0-300	282	20	288	15.5-58.5	(Mahbubul *et al*. 2015b)
0.100	0	0.000	7.0	74-87	61-661	100	20	295	28.2-51.4	(Zhu *et al*. 2011)
0.100	0	0.000	6.0	30	0-1807	700	40	300	22.2-34.5	(Jang *et al*. 2007)
0.050	0	0.000	7.0	105-134	59-300	400	20	298	55-58.4	(Mahbubul *et al*. 2015a)
0.050	3	0.050	2.8-10.2	242-312	15	100	40	298	28.7-39.1	(Wang and Zhu 2009)
0.050	3	0.050	1-9.1	207	15	100	40	300	29.2-40.7	(Zhu *et al*. 2009)
0.050	3, 4	0.02-0.18	1-10.7	38-207	15	100	40	298-300	28.8-39.9	(Wang *et al*. 2011)
0.01-0.8	0	0.000	2.4-12.1	40	60-180	750	19	298	33.8-50.3	(Choudhary *et al*. 2017)
0.5-3	0	0.000	7.0	108-588	0-40505	200	24	308	25-57.8	(Sadeghi *et al*. 2015)
0.13-0.65	0	0.000	5.3-6.6	160-208	30	250	23	298	11.8-14.3	(Wang and Wang 2017)
0.5-1	0	0.000	7.2-7.5	20	60	200	24	298	46.7-51.3	(Lai *et al*. 2009)
0.200	0	0.000	2.6-11.4	6	120	100	40	298	21.1-50.5	(Syarif and Prajitno 2015)
0.030	0	0.000	1.1-10	115-120	20	500	20	298	21.3-34.3	(Cacua *et al*. 2019)
0.01-0.03	0	0.000	44239.0	68-1066	10	200	20	298	27.5-55.1	(Zareei *et al*. 2019)
0.115-0.98	0	0.000	7.0	22-101	240	600	40	320	20.1-30.1	(Liu *et al*. 2019)
0.100	0	0.000	7.0	60-84	61-660	100	20	310	28.1-52	(Zhao *et al*. 2011)
0.050	0	0.000	2.1-12.9	45	360	200	20	298	39.2-50.4	(Pastoriza-Gallego *et al*. 2009)
0.471-1.27	0	0.000	7.0	127-163	180	100	60	298	32.3-49	(Hung *et al*. 2013)
0.010	0	0.000	7.2	20	63-187	100	40	298	26.4-41.7	(Lu *et al*. 2015)
0.003-0.257	0	0.000	7.0	40	240	600	40	293	22.7-45.1	(Pare and Ghosh 2019)
0.003-0.01	0	0.000	7.0	575	40	290	40	298	40.5-53.8	(Vakilinejad *et al*. 2021)
0.100	0	0.000	7.0	60-84	120-901	100	20	298	28.2-52	(Zhao *et al*. 2009)
0.05-0.2	0	0.000	2.0-12	29	510	400	24	298	32.8-34.8	(Okonkwo *et al*. 2020)
0.010	0	0.000	1.1-12	50	350-360	110	50	297	46-51.3	(Lee 2013)
0.100	0	0.000	4.1	10-150	300	150	60	298	42.8-57.4	(Hyungjoon Kim 2016)
0.125-1.5	1,2	0.020	7-7.7	25	180	50	40	298	31.4-42.6	(Mukherjee *et al*. 2020)
0.100	3	0.11-0.993	1.1-10.7	130	60	100	40	298	28.8-39.8	(Wang *et al*. 2008)
0.100	3	0.171-0.713	8.5	138-253	60	100	40	298	29.6-38.9	(Zhu *et al*. 2008)

F1: Nano-alumina concentration in water (volume percent)
F2: Surfactant type, i.e., no surfactant (0), Polyvinylalcohol (1), Polyvinylpyrrolidone (2), Sodium Dodecylbenzene Sulfonate (3), and Sodium dodecyl sulfate (4)
F3: Surfactant concentration (weight percent)
F4: pH value
F5: Nano-alumina diameter (nm)
F6: Ultrasonic agitation time (min)
F7: Ultrasonic power (W)
F8: Ultrasonic frequency (kHz)
F9: Temperature (K)
R1: Zeta potential (mV)

frequency, and duration), surfactant information (type and concentration), and nanoparticle size. It should be mentioned that the stability regimes of all experimental datasets belong to either first to fourth classes (i.e., classes 1 to 4), and no dataset is available for excellent stability of alumina-water nanofluids (i.e., class 5).

The development and validation phases of the artificial intelligent classifiers have been conducted using this experimental databank. Then it is possible to rank the classifiers based on their classification accuracies.

2.3 Artificial intelligent classifiers

Machine learning techniques are among the most popular methods for damage detection in concrete (Dauji 2020), plates (Saadatmorad *et al*. 2021) and composites (Khatir *et al*. 2019, Khatir *et al*. 2021, Zenzen *et al*. 2020), characterizing composites (Guo and Yang 2020, Wang *et al*. 2022) and cement-based materials (Al-Musawi *et al*. 2020, Jalal *et al*. 2020, Mazloom *et al*. 2020, Nguyen *et al*. 2020). They also successfully applied to parameter approximation

(Yousefi *et al*. 2020, Amidi *et al*. 2021) purposes, like crack identification in plates (Khatir *et al*. 2020), pipelines (Seguini *et al*. 2021), and composites (Tran-Ngoc *et al*. 2021), study movement the landslide (Luo *et al*. 2020), flexure stiffness of FGM beams (Madenci and Gulcu 2020), receding contact issue (Yaylacı *et al*. 2020), and financial markets analysis (Charandabi and Kamyar 2021a, b).

In this study, five different intelligent classifiers, i.e., deep learning (Yan *et al*. 2021, Podder*et al*. 2020), multilayer perceptron neural network (Daryayehsalameh *et al*. 2021, Cao *et al*. 2021), decision tree (Myles *et al*. 2004), GoogleNet (Alizadeh *et al*. 2021), and multi-output least squares support vector regression (Moosavi *et al*. 2021, Karimi *et al*. 2021) have been employed to estimate the stability regimes of alumina-water nanofluids. The two non-overlapping groups, i.e., training and testing (90:10), are randomly selected from the collected datasets. Indeed, 311 experimental datasets are devoted to the training group, and the 34 remaining ones are considered as a testing group.

As its name shows, the first group is responsible for engaging in the learning phase to help an optimization technique adjust the hyper-parameters of the considered classifiers. During the learning phase, all classifiers are provided with independent variables and the stability regime of alumina-water nanofluids. On the other hand, the hyper-parameters of the classifiers are unknown, and an optimization algorithm adjusts them by minimizing a pre-defined objective function.

The second group is then employed to evaluate the classification accuracy of the trained classifier encountering some unknown situations. More specifically, the trained classifiers in the testing phase are only allowed to receive the independent variables. In this way, their accuracy can be measured using situations that were not seen previously.

Generally, a classifier is finally selected as the best one differentiating among stability regimes of both training and testing groups with acceptable accuracy. The classification accuracy of all considered models in the training and testing phases is measured and compared, and the most reliable one is introduced.

3. Results and discussion

As mentioned earlier, the classification accuracy of the considered machines in the training and testing phases is the main criterium to choose the best model for differentiating among stability regimes of the alumina-water nanofluids. Classification accuracy (CA) and misclassification percent (MCP) can be calculated using Eqs. (1) and (2), respectively (Vaferi *et al*. 2016).

$$CA(\%)=100\times\frac{Numbers\,of\,correct\,detection}{Total\,numbers\,of\,datasets} \quad (1)$$

$$MCP(\%)=100-CA \quad (2)$$

3.1 The most reliable classifier

Fig. 2 depicts the ranking order of the considered artificial intelligent classifiers for deafferenting among stability regimes of the alumina-water nanofluids. As previously explained, the MLPNN, MLS-SVR, deep learning neural network, GoogleNet, and decision tree are the first to fifth accurate classifiers, respectively.

Before here, a combination of the trial-and-error and ranking anlyses approved that the MLPNN is the most efficient model to classify the stability regimes of water-

Table 3 Classification accuracy of the considered models for learning and testing phases

Intelligent classifier	Classification accuracy (%)		
	Train	Test	Overall
Deep learning neural networks	76.53	52.94	74.20
Decision tree	24.44	26.47	24.64
GoogleNet	63.98	58.82	63.48
Multilayer perceptron neural networks	**87.78**	**70.59**	**86.09**
Multi-output least squares support vector regression	79.10	61.76	77.40

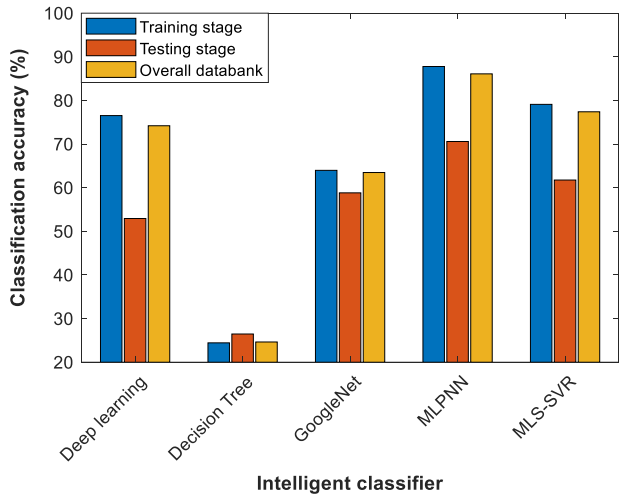

Fig. 1 Classification accuracy of the considered models for learning and testing phases

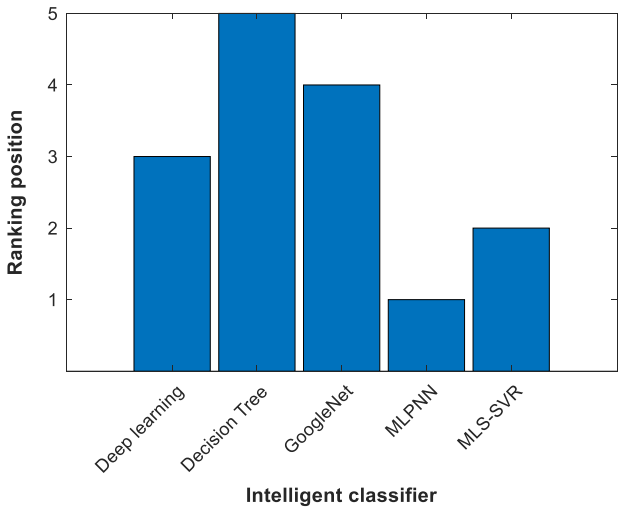

Fig. 2 Results of ranking analysis of classification accuracy of the considered models (MLPNN is the best and decision tree is the worst classifier)

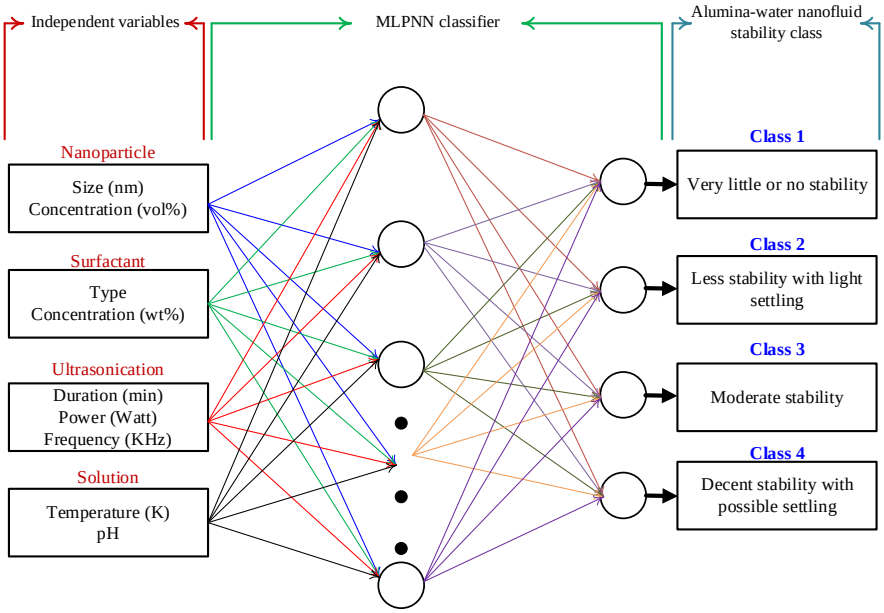

Fig. 3 Structure of the developed MLPNN to differentiate among stability regimes of the alumina-water nanofluids

alumina nanofluids. Therefore, it is better to explain the mathematical and working process of the multilayer perceptron neural networks (see Appendix).

3.2 Determining structural features of the MLPNN classifier

The schematic of the developed MLPNN classifier for differentiating among stability regimes of the alumina-water nanofluids is given in Fig. 3.

This figure explains that the engineered MLPNN classifier only needs nanoparticle, surfactant, ultrasonic, and nano-suspension characteristics to predict the stability regime of the alumina-water nanofluids. Since none of the collected databases have a Zeta potential of higher than 45 mV, the MLPNN output is only valid for detecting the first fourth classes.

3.2.1 Finding the best training algorithm

It was previously stated that an optimization algorithm uses the training datasets to adjust the hyper-parameters of a given classifier. Since the learning phase is a central processing stage for developing any intelligent classifiers, this section investigates the effect of the optimization algorithm on the classification accuracy of the MLPNN model. Table 4 presents the accuracy of the MLPNN classifiers trained by eleven optimization algorithms in the training and testing phases. The overall classification accuracies are also summarized in this table. Table 4 shows that the Bayesian regularization backpropagation is the best optimization algorithm for training the MLPNN classifier. Adjusting the MLPNN parameters using this algorithm results in the classification accuracy of 88.42% (training phase), 76.47% (testing phase), and 87.25% (all databank). On the other hand, both gradient descent and gradient descent with momentum backpropagation algorithms are the worst optimization techniques for training the MLPNN classifier. It is worth noting that the structure of the MLPNN classifier (i.e., 9-9-4) and its output layer activation function (i.e., logarithm sigmoid) are constant in this analysis.

Table 4 Effect of the optimization algorithms on the classification accuracy of the MLPNN

Optimization algorithm	Classification accuracy (%)		
	Train	Test	Overall
Bayesian regularization backpropagation	**88.42**	**76.47**	**87.25**
Gradient descent with adaptive learning rate backpropagation	71.38	70.59	71.30
Conjugate gradient backpropagation with Powell-Beale restarts	80.71	64.71	79.13
Conjugate gradient backpropagation with Polak-Ribiére updates	81.03	70.59	80.00
Levenberg-Marquardt backpropagation	87.78	70.59	86.09
Gradient descent with momentum and adaptive learning rate	69.45	55.88	68.12
Scaled conjugate gradient backpropagation	83.92	76.47	83.19
Resilient backpropagation	83.28	70.59	82.03
One-step secant backpropagation	77.17	70.59	76.52
Gradient descent backpropagation	46.30	47.06	46.38
Gradient descent with momentum backpropagation	46.30	47.06	46.38

3.2.2 The best activation function

It is customary to show the correct class by one and incorrect ones by zero in the classification study (Vaferi *et al*. 2016). Therefore, there are limited numbers of activation functions that can be placed in the output layer of the MLPNN classifier. Indeed, only the logarithm sigmoid, linear, SoftMax, hard-limit, and saturating linear satisfy this requirement. Therefore, this stage investigates the effect of the output layer activation function on the MLPNN

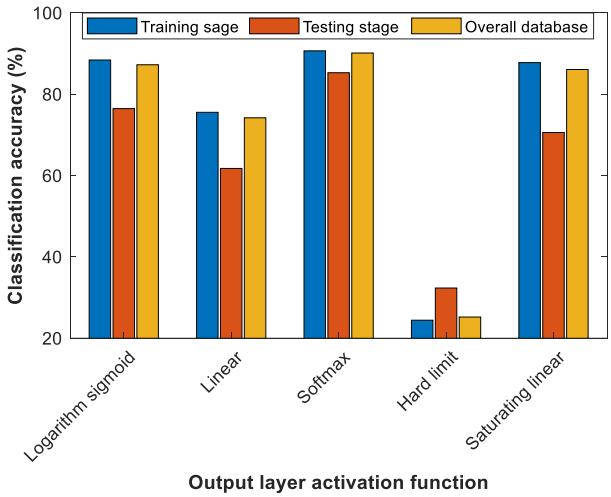

Fig. 4 Effect of output layer transfer function on the classification accuracy of the MLPNN

Table 5 Effect of output layer transfer function on the classification accuracy of the MLPNN

Output layer transfer function	Classification accuracy (%)		
	Training	Testing	Whole data
Logarithm sigmoid	88.42	76.47	87.25
Linear	75.56	61.76	74.21
Softmax	**90.67**	**85.29**	**90.14**
Hard limit	24.44	32.354	25.22
Saturating linear	87.78	70.59	86.09

Table 6 A typical confusion matrix for a two-class classification problem

		Estimated	
		Positive	**Negative**
Target	**Positive**	True-positive (**TP**)	False-negative (**FN**)
	Negative	False-positive (**FP**)	True-negative (**TN**)

Table 7 A typical confusion matrix covering a four-class classification problem

TP class 1	FP class 2	FP class 3	FP class 4	TPR class 1 FNR class 1
FP class 1	TP class 2	FP class 3	FP class 4	TPR class 2 FNR class 2
FP class 1	FP class 2	TP class 3	FP class 4	TPR class 3 FNR class 3
FP class 1	FP class 2	FP class 3	TP class 4	TPR class 4 FNR class 4
PPV class 1 FDR class 1	PPV class 2 FDR class 2	PPV class 3 FDR class 3	PPV class 4 FDR class 4	Overall CA Overall MCA

classification success. Fig. 4 illustrates the classification accuracy of MLPNN-based classifiers equipped with different activation functions in the training, testing, and all databases. Although the logarithm sigmoid and SoftMax activation functions show relatively similar performances, Table 5 shows that the latter provides the MLPNN with the best accuracy for estimating the training, testing, and all databases.

In summary, the MLPNN model (with the 9-9-4 structure and SoftMax activation function in the output layer) trained by the Bayesian regularization back-propagation algorithm is the best classifier for identifying stability regimes of the alumina-water nanofluids. This intelligent classifier accurately detects more than 90% of the stability regimes of 345 nanofluid samples.

3.3 Performance evaluation of the MLPNN classifier

Despite the regression study that often relies on statistical accuracy criteria such as mean square error to evaluate the performance of a designed model (Jiang *et al.* 2021), the efficiency of classifiers is often measured using the confusion matrix (Vaferi *et al.* 2016). Table 6 shows a typical confusion matrix for a binary classification problem.

The confusion matrix presents the numbers of true-positive (TP), true-negative (TN), false-positive (FP), and false-negative (FN) results of a given classifier.

Then, it is possible to measure a classifier performance using the true-positive rate (TPR), false-negative rate (FNR), positive predictive value (PPV), and false discovery rate (FDR) indices. Eqs. (3)-(6) present the mathematical formula of these indices (Alizadeh *et al.* 2021).

$$TPR(\%)=100\times\frac{TP}{TP+FN} \tag{3}$$

$$FNR(\%)=100\times\frac{FN}{TP+FN}=100-TPR \tag{4}$$

$$PPV(\%)=100\times\frac{TP}{TP+FP} \tag{5}$$

$$FDR(\%)=100\times\frac{FP}{TP+FP}=100-PPV \tag{6}$$

As mentioned earlier, identifying alumina-water nanofluid stability regimes is a four-class classification problem. As Table 7 shows, the confusion matrix often contains the numbers of true-positive and false-positive identifications, TPR, FNR, PPV, FDR, overall classification accuracy, and misclassification percent. It is worth noting that since TN and FN can be easily calculated from the TP and FP values, there is no need to present them in the confusion matrix.

From the classification perspective, it is better to develop a classifier that allocates high values for both TPR and PPV indices (as close as possible to 100). It also means that the classifier assigns small values to both FNR and

FDR criteria (as close as possible to zero). Indeed, the minimum value for the false-negative and false-positive indicators is preferred.

Figs. 5-7 present the obtained confusion matrices by the MLPNN model for the training, testing, and all databases, respectively. Fig. 5 shows that the MLPNN classifier presents the TPR and PPV values higher than 90% for all training classes, excluding the second class. The designed MLPNN encounters some difficulty in correctly detecting

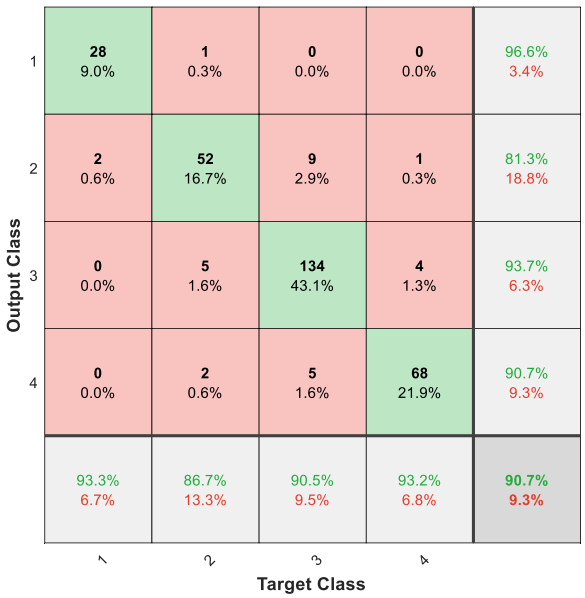

Fig. 5 Confusion matrix of the MLPNN classifier for the training phase

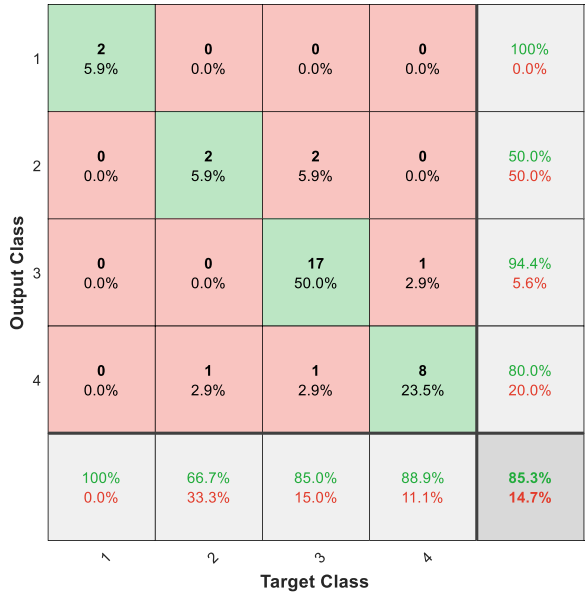

Fig. 6 Performance of the MLPNN during the testing stage

the second stability class. The TPR = 81.3% and PPV = 86.7% have been achieved for classifying the second stability regime of alumina-water nanofluids. Fig. 5 also shows that the proposed MLPNN model successfully detects the correct stability regimes of 90.7% of the training group (282 out of 311 samples).

The confusion matrix provided by the MLPNN model for classifying the stability regimes of 34 water-alumina samples in the testing stage is shown in Fig. 6. Since the developed MLPNN classifier does not previously see the testing data, its performance is expected to be weaker than the training phase. Like the training stage, the MLPNN model experiences difficulties in correctly distinguishing the second stability regime of alumina-water nanofluids.

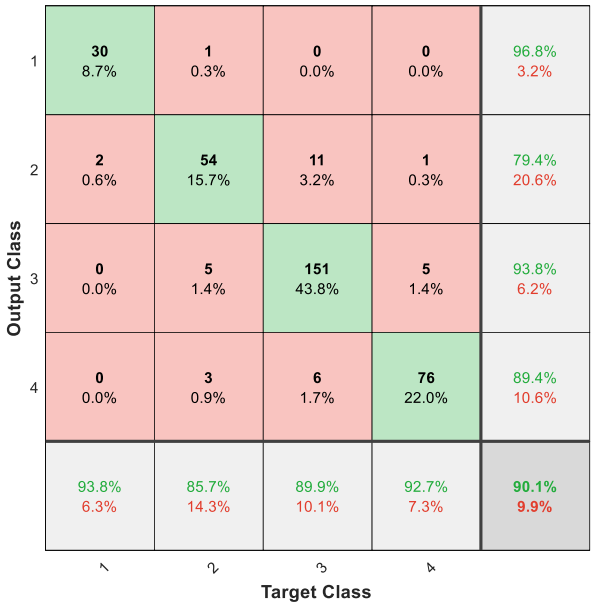

Fig. 7 The efficiency of the MLPNN for differentiation among stability regimes of the alumina-water nanofluids (overall datasets)

The MLPNN model accurately detects the first to the fourth stability regimes with the TPR of 100%, 50%, 94.4%, and 80%, respectively. The total classification accuracy and misclassification percent of the MLPNN model in the testing stage is 85.3% and 14.7%.

The confusion matrix for the all database that is a weighted average of the training and testing phases is exhibited in Fig. 7. Excluding the second class, the MLPNN model successfully differentiates among the stability regimes with a classification accuracy of ~90%. It should be mentioned that the MLPNN performance for classifying the second stability regime (i.e., TPR=79.4% and PPV=85.7%) is also at an acceptable level. Since the MLPNN model shows the weakest efficiency for identifying the second class, it is better to highlight this.

The overall classification accuracy and misclassification percent for 345 water-alumina samples are 90.1% and 9.9%, respectively.

4. Conclusions

The current study looks at the stability regime of water-alumina nano-suspension as a classification problem. Five well-known artificial intelligent classifiers have been applied to detect the stability dependency on the nanoparticle, suspension, ultrasonic agitation, and surfactant characteristics. The classification accuracies of the intelligent models (deep learning and multilayer perceptron neural networks, decision tree, GoogleNet, and MLS-SVR) were compared to find the most reliable one. Combining the ranking analyses and the classification accuracy approved that the trained MLPNN model (9-9-4 structure and SoftMax activation function in the output layer) by the Bayesian regularization backpropagation algorithm is the best choice for the considered task. The MLPNN model

with the optimum structure detects the correct stability regime of more than 90% of 345 water-alumina samples. Our proposed model can be readily used to determine the operating conditions that result in a stable alumina-water nanofluid. This MLPNN classifier not only saves time also reduces the experimental cost.

References

Abid, N., Ramzan, M., Chung, J.D., Kadry, S. and Chu, Y.M. (2020), "Comparative analysis of magnetized partially ionized copper, copper oxide–water and kerosene oil nanofluid flow with Cattaneo–Christov heat flux", *Sci. Rep. UK.*, **10**(1), 1-14. https://doi.org/10.1038/s41598-020-74865-5.

Alibak, A.H., Khodarahmi, M., Fayyazsanavi, P., Alizadeh, S.M., Hadi, A.J. and Aminzadehsarikhanbeglou, E. (2022), "Simulation the adsorption capacity of polyvinyl alcohol/ carboxymethyl cellulose based hydrogels towards methylene blue in aqueous solutions using cascade correlation neural network (CCNN) technique", *J. Clean. Prod.*, **337**, 130509. https://doi.org/10.1016/j.jclepro.2022.130509.

Ali, V., Ibrahim, M., Berrouk, A.S., Algehyne, E.A., Saeed, T. and Chu, Y.M. (2021), "Navigating the effect of tungsten oxide nano-powder on ethylene glycol surface tension by artificial neural network and response surface methodology", *Powder Technol.*, **386**, 483-490. https://doi.org/10.1016/j.powtec.2021.03.043.

Alizadeh, S.M., Khodabakhshi, A., Abaei Hassani, P. and Vaferi, B. (2021), "Smart-identification of petroleum reservoir well testing models using deep convolutional neural networks (GoogleNet)", *J. Energ. Resour. Technol.*, **143**(7), 073008. https://doi.org/10.1115/1.4050781.

Al-Musawi, A.A., Alwanas, A.A., Salih, S.Q., Ali, Z.H., Tran, M.T. and Yaseen, Z.M. (2020), "Shear strength of SFRCB without stirrups simulation: implementation of hybrid artificial intelligence model", *Eng. Comput. Germany.*, **36**(1), 1-11. https://doi.org/10.1007/s00366-018-0681-8.

Amidi, Y., Nazari, B., Sadri, S. and Yousefi, A. (2021), "Parameter estimation in multiple dynamic synaptic coupling model using bayesian point process state-space modeling framework", *Neural Comput.*, **33**(5), 1269-1299. http://doi.org/10.1162/neco_a_01375.

Angayarkanni, S.A. and Philip, J. (2014), "Effect of nanoparticles aggregation on thermal and electrical conductivities of nanofluids", *J. Nanofluids.*, **3**(1), 17-25. https://doi.org/10.1166/jon.2014.1083.

Arani, A.G., Farazin, A. and Mohammadimehr, M. (2021), "The effect of nanoparticles on enhancement of the specific mechanical properties of the composite structures: A review research", *Adv nano Res.*, **10**(4), 327-337. http://doi.org/10.12989/anr.2021.10.4.327.

Asadi, A., Bakhtiyari, A.N. and Alarifi, I.M. (2021), "Predictability evaluation of support vector regression methods for thermophysical properties, heat transfer performance, and pumping power estimation of MWCNT/ZnO-engine oil hybrid nanofluid", *Eng. Comput. Germany.*, **37**(4), 3813-3823. https://doi.org/10.1007/s00366-020-01038-3.

Baláž, M., Balážová, Ľ., Kováčová M., Daneu, N., Salayova, A., Bedlovičová, Z. and Tkáčiková, Ľ. (2019), "The relationship between precursor concentration and antibacterial activity of biosynthesized Ag nanoparticles", *Adv. Nano. Res.*, **7**(2), 125-134. http://doi.org/10.12989/anr.2019.7.2.125.

Bao, L., Zhong, C., Jie, P. and Hou, Y. (2019), "The effect of nanoparticle size and nanoparticle aggregation on the flow characteristics of nanofluids by molecular dynamics simulation", *Adv. Mech. Eng.*, **11**, 1687814019889486. https://doi.org/10.1177/1687814019889486.

Cacua, K., Ordoñez, F., Zapata, C., Herrera, B., Pabón, E. and Buitrago-Sierra, R. (2019), "Surfactant concentration and pH effects on the zeta potential values of alumina nanofluids to inspect stability", *Colloid Surface A*, **583**, 123960. https://doi.org/10.1016/j.colsurfa.2019.123960.

Cao, Y., Kamrani, E., Mirzaei, S., Khandakar, A. and Vaferi, B. (2022), "Electrical efficiency of the photovoltaic/thermal collectors cooled by nanofluids: Machine learning simulation and optimization by evolutionary algorithm", *Energy Rep.*, **8**, 24-36. https://doi.org/10.1016/j.egyr.2021.11.252.

Charandabi, S.E. and Kamyar, K. (2021a), "Prediction of cryptocurrency price index using artificial neural networks: A survey of the literature", *Eur. J. Bus. Man Res.*, **6**(6), 17-20. https://doi.org/10.24018/ejbmr.2021.6.6.1138.

Charandabi, S.E. and Kamyar, K. (2021b), "Using a feed forward neural network algorithm to predict prices of multiple cryptocurrencies", *Eur. J. Bus. Man Res.*, **6**(5), 15-19. https://doi.org/10.24018/ejbmr.2021.6.5.1056.

Choudhary, R., Khurana, D., Kumar, A. and Subudhi, S. (2017), "Stability analysis of Al_2O_3/water nanofluids", *J. Exp. Nanosci.*, **12**, 140-151. https://doi.org/10.1080/17458080.2017.1285445.

Chu, Y.M., Ali, R., Asjad, M.I., Ahmadian, A. and Senu, N. (2020a), "Heat transfer flow of Maxwell hybrid nanofluids due to pressure gradient into rectangular region", *Sci. Rep. UK.*, **10**(1), 1-18. https://doi.org/10.1038/s41598-020-73174-1.

Chu, Y.M., Ikram, M.D., Asjad, M.I., Ahmadian, A. and Ghaemi, F. (2021), "Influence of hybrid nanofluids and heat generation on coupled heat and mass transfer flow of a viscous fluid with novel fractional derivative", *J. Therm. Anal. Calorim.*, **144**, 2057-2077. https://doi.org/10.1007/s10973-021-10692-8.

Chu, Y.M., Kumar, R. and Bach, Q.V. (2020b), "Water-based nanofluid flow with various shapes of Al_2O_3 nanoparticles owing to MHD inside a permeable tank with heat transfer", *Appl. Nanosci.*, 1-12. https://doi.org/10.1007/s13204-020-01609-2.

Daryayehsalameh, B., Nabavi, M. and Vaferi, B. (2021), "Modeling of CO_2 capture ability of [Bmim][BF_4] ionic liquid using connectionist smart paradigms", *Environ. Technol. Innov.*, **22**, 101484. https://doi.org/10.1016/j.eti.2021.101484.

Dauji, S. (2020), "Prediction of concrete spall damage under blast: Neural approach with synthetic data", *Comput. Concrete.*, **26**(6), 533-546. https://doi.org/10.12989/cac.2020.26.6.533.

Deng, X., Yang, T., Zhang, Q., Chu, Y., Luo, J., Zhang, L. and Li, P. (2019), "A monolith CuNiFe/γ-Al_2O_3/Al catalyst for steam reforming of dimethyl ether and applied in a microreactor", *Int. J. Hydrogen. Energ.*, **44**(5), 2417-2425. https://doi.org/10.1016/j.ijhydene.2018.11.072.

Ebadian, M.A. and Lin, C.X. (2011), "A review of high-heat-flux heat removal technologies", *J Heat Transfer.*, **133**, 110801. https://doi.org/10.1115/1.4004340.

Esfe, M.H., Esfandeh, S. and Bahiraei, M. (2020), "A two-phase simulation for investigating natural convection characteristics of nanofluid inside a perturbed enclosure filled with porous medium", *Eng. Comput. Germany.*, 1-18. https://doi.org/10.1007/s00366-020-01204-7.

Esmaeili-Faraj, S.H., Hassanzadeh, A., Shakeriankhoo, F., Hosseini, S. and Vaferi, B. (2021), "Diesel fuel desulfurization by alumina/polymer nanocomposite membrane: Experimental analysis and modeling by the response surface methodology", *Chem. Eng. Process.*, **164**, 108396. https://doi.org/10.1016/j.cep.2021.108396.

Ghadimi, A. (2013), "Stability and thermal conductivity of low concentration titania nanofluids", Ph.D. Dissertation, Universiti Malaya, Kuala Lumpur, Malaysia.

Gul, N., Ramzan, M., Chung, J.D., Kadry, S. and Chu, Y.M.

(2020), "Impact of hall and ion slip in a thermally stratified nanofluid flow comprising Cu and Al_2O_3 nanoparticles with nonuniform source/sink", *Sci. Rep. UK.*, **10**(1), 1-18. https://doi.org/10.1038/s41598-020-74510-1.

Guo, K. and Yang, G. (2020), "Load-slip curves of shear connection in composite structures: Prediction based on ANNs", *Steel. Compos. Struct.*, **36**(5), 493-506. https://doi.org/10.12989/scs.2020.36.5.493.

Haq, F., Khan, M.I., Chu, Y.M., Khan, N.B. and Kadry, S. (2021), "Non-magnetized mixed convective viscous flow submerged in titanium oxide and aluminum titanium oxide hybrid nanoparticles towards a surface of cylinder", *Int. Commun. Heat Mass.*, **120**, 105027. https://doi.org/10.1016/j.icheatmasstransfer.2020.105027.

Huang, J., Wang, X., Long, Q., Wen, X., Zhou, Y. and Li, L. (2009), "Influence of pH on the stability characteristics of nanofluids", *Proceedings of the Symposium on Photonics and Optoelectronics*, Wuhan, China, August.

Hungjoon, K. (2016), "Effective dynamic conductivity correlation of nanofluids in convective flow", Ph.D. Dissertation, Seoul National University, Seoul.

Hung, Y.H., Chen, J.H. and Teng, T.P. (2013), "Feasibility assessment of thermal management system for green power sources using nanofluid", *J. Nanomater.*, **2013**, 321261. https://doi.org/10.1155/2013/321261.

Ibrahim, M., Algehyne, E.A., Saeed, T., Berrouk, A.S. and Chu, Y.M. (2021), "Study of capabilities of the ANN and RSM models to predict the thermal conductivity of nanofluids containing SiO_2 nanoparticles", *J. Therm. Anal. Calorim.*, **145**, 1993-2003. https://doi.org/10.1007/s10973-021-10674-w.

İpek, S. and Mermerdaş, K. (2020), "Experimental and computational study on fly ash and kaolin based synthetic lightweight aggregate", *Comput. Concrete.*, **26**(4), 327-342. https://doi.org/10.12989/cac.2020.26.4.327.

Iqbal, W., Jalil, M., Khadimallah. M.A., Hussain, M., Naeem, M.N., Al Naim, A.F. and Tounsi, A. (2021), "Interaction of casson nanofluid with Brownian motion: Temperature profile with shooting method", *Adv. Nano. Res.*, **10**(4), 349-357. https://doi.org/10.12989/anr.2021.10.4.349.

Jalal, M., Grasley, Z., Gurganus, C. and Bullard, J.W. (2020), "A new nonlinear formulation-based prediction approach using artificial neural network (ANN) model for rubberized cement composite", *Eng. Comput. Germany.*, 1-18. https://doi.org/10.1007/s00366-020-01054-3.

Jang, S.P., Hwang, K.S., Lee, J.H., Kim, J.H., Lee, B.H. and Choi, S.U. (2007), "Effective thermal conductivities and viscosities of water-based nanofluids containing Al_2O_3 with low concentration", *Proceddings of the 7th IEEE Conference on Nanotechnology (IEEE NANO)*, Hong Kong, China, August.

Jiang, Y., Zhang, G., Wang, J. and Vaferi, B. (2021), "Hydrogen solubility in aromatic/cyclic compounds: Prediction by different machine learning techniques", *Int. J. Hydrogen Energy.*, **46**, 23591-23602. https://doi.org/10.1016/j.ijhydene.2021.04.148.

Kaabipour, S. and Hemmati, S. (2021), "A review on the green and sustainable synthesis of silver nanoparticles and one-dimensional silver nanostructures", *Beilstein J. Nanotech.*, **12**(1), 102-136. https://doi.org/10.3762/bjnano.12.9.

Kang, H., Zhang, Y., Yang, M. and Li, L. (2012), "Molecular dynamics simulation on effect of nanoparticle aggregation on transport properties of a nanofluid", *J. Nanotechnol. Eng. Med.*, **3**, 021001. https://doi.org/10.1115/1.4007044.

Karimi, M., Aminzadehsarikhanbeglou, E. and Vaferi, B. (2021), "Robust intelligent topology for estimation of heat capacity of biochar pyrolysis residues", *Measurement.*, **183**, 109857. https://doi.org/10.1016/j.measurement.2021.109857.

Kazemi, M.H. and Nasr, M.A.B.M. (2014), "Convective heat transfer of MWCNT/HT-B Oil nanofluid inside micro-fin helical tubes under uniform wall temperature condition", *Adv. Nano Res.*, **2**(2), 99-109. https://doi.org/10.12989/anr.2014.2.2.099.

Keshtkar, Z., Tamjidi, S. and Vaferi, B. (2021), "Intensifying nickel (II) uptake from wastewater using the synthesized γ-alumina: An experimental investigation of the effect of nano-adsorbent properties and operating conditions", *Environ. Technol. Innov.*, **22**, 101439. https://doi.org/10.1016/j.eti.2021.101439.

Khalifeh, A. and Vaferi, B. (2019), "Intelligent assessment of effect of aggregation on thermal conductivity of nanofluids-Comparison by experimental data and empirical correlations", *Thermochim. Acta.*, **681**, 178377. https://doi.org/10.1016/j.tca.2019.178377.

Khan, M.I., Qayyum, S., Farooq, S., Chu, Y.M. and Kadry, S. (2021), "Modeling and simulation of micro-rotation and spin gradient viscosity for ferromagnetic hybrid (Manganese Zinc Ferrite, Nickle Zinc Ferrite) nanofluids", *Math. Comput. Simulat.*, **185**, 497-509. https://doi.org/10.1016/j.matcom.2021.01.007.

Khatir, S., Boutchicha, D., Le Thanh, C., Tran-Ngoc, H., Nguyen, T.N. and Wahab, M.A. (2020), "Improved ANN technique combined with Jaya algorithm for crack identification in plates using XIGA and experimental analysis", *Theor. Appl. Fract Mec.*, **107**, 102554. https://doi.org/10.1016/j.tafmec.2020.102554.

Khatir, S., Tiachacht, S., Le Thanh, C., Ghandourah, E., Mirjalili, S. and Wahab, M.A. (2021), "An improved artificial neural network using arithmetic optimization algorithm for damage assessment in FGM composite plates", *Compos. Struct.*, **273**, 114287. https://doi.org/10.1016/j.compstruct.2021.114287.

Khatir, S., Tiachacht, S., Thanh, C.L., Bui, T.Q. and Wahab, M.A. (2019), "Damage assessment in composite laminates using ANN-PSO-IGA and Cornwell indicator", *Compos. Struct.*, **230**, 111509. https://doi.org/10.1016/j.compstruct.2019.111509.

Kole, M. and Dey, T.K. (2011), "Effect of aggregation on the viscosity of copper oxide-gear oil nanofluids", *Int. J. Therm. Sci.*, **50**, 1741-1747. https://doi.org/10.1016/j.ijthermalsci.2011.03.027.

Lai, W.Y., Vinod, S., Phelan, P.E. and Prasher, R. (2009), "Convective heat transfer for water-based alumina nanofluids in a single 1.02-mm tube", *J. Heat Transfer.*, **131**, 112401. https://doi.org/10.1115/1.3133886.

Lee, S.W. (2013), "Effects of Graphene and SiC nanofluids on critical heat flux and quenching for advanced nuclear reactors", Ph.D. Dissertation, Ulsan National Institute of Science and Technology, Ulsan, Korea.

Liu, L., Stetsyuk, V., Kubiak, K.J., Yap, Y.F., Goharzadeh, A. and Chai, J.C. (2019), "Nanoparticles for convective heat transfer enhancement: Heat transfer coefficient and the effects of particle size and zeta potential", *Chem. Eng. Commun.*, **206**, 761-771. https://doi.org/10.1080/00986445.2018.1525364.

Li, X., Chen, Y., Mo, S., Jia, L. and Shao, X. (2014), "Effect of surface modification on the stability and thermal conductivity of water-based SiO_2-coated graphene nanofluid", *Thermochim. Acta.*, **595**, 6-10. https://doi.org/10.1016/j.tca.2014.09.006.

Luo, Z., Luo, Z., Qin, Y., Wen, L., Ma, S. and Dai, Z. (2020), "Developing new tree expression programing and artificial bee colony technique for prediction and optimization of landslide movement", *Eng. Comput. Germany.*, **36**(3), 1117-1134. https://doi.org/10.1007/s00366-019-00754-9.

Lu, S., Song, J., Li, Y., Xing, M. and He, Q. (2015), "Improvement of CO_2 absorption using Al_2O_3 nanofluids in a stirred thermostatic reactor", *Can. J. Chem. Eng.*, **93**, 935-941. https://doi.org/10.1002/cjce.22175.

Madenci, E. and Gulcu, S. (2020), "Optimization of flexure stiffness of FGM beams via artificial neural networks by mixed

FEM", *Struct*. *Eng*. *Mech*., **75**(5), 633-642. https://doi.org/10.12989/sem.2020.75.5.633.

Mahajan, S. (2017), "Study of stability and thermal conductivity of nanoparticles in propylene glycol", M.Sc. Thesis, Minnesota State University, Mankato, U.S.A.

Mahbubul, I.M., Saidur, R., Amalina, M.A., Elcioglu, E.B. and Okutucu-Ozyurt, T. (2015a), "Effective ultrasonication process for better colloidal dispersion of nanofluid", *Ultrason Sonochem*., **26**, 361-369. https://doi.org/10.1016/j.ultsonch.2015.01.005.

Mahbubul I.M., Shahrul I.M., Khaleduzzaman S.S., Saidur, R., Amalina, M.A. and Turgut, A.L.P.A.S.L.A.N. (2015b), "Experimental investigation on effect of ultrasonication duration on colloidal dispersion and thermophysical properties of alumina-water nanofluid", *Int. J. Heat Mass Transf*., **88**, 73-81. https://doi.org/10.1016/j.ijheatmasstransfer.2015.04.048.

Mazloom, M., Tajar, S.F. and Mahboubi, F. (2020), "Long-term quality control of self-compacting semi-lightweight concrete using short-term compressive strength and combinatorial artificial neural networks", *Comput*. *Concrete*., **25**(5), 401-409. https://doi.org/10.12989/cac.2020.25.5.401.

Moosavi, S.R., Vaferi, B. and Wood, D.A. (2021), "Auto-characterization of naturally fractured reservoirs drilled by horizontal well using multi-output least squares support vector regression", *Arab*. *J*. *Geosci*., **14**, 545. https://doi.org/10.1007/s12517-021-06559-9.

Mukherjee, S., Chakrabarty, S., Mishra, P.C. and Chaudhuri, P. (2020), "Transient heat transfer characteristics and process intensification with Al_2O_3-water and TiO_2-water nanofluids: An experimental investigation", *Chem*. *Eng*. *Process*., **150**, 107887. https://doi.org/10.1016/j.cep.2020.107887.

Mukherjee, S., Mishra, P.C. and Chaudhuri, P. (2018), "Stability of heat transfer nanofluids-a review", *ChemBioEng Rev*., **5**, 312-333. https://doi.org/10.1002/cben.201800008.

Myles, A.J., Feudale, R.N., Liu, Y., Woody, N.A. and Brown, S.D. (2004), "An introduction to decision tree modeling", *J*. *Chemomometrics*, **18**, 275-285. https://doi.org/10.1002/cem.873.

NawazishMehdia S., Hussain M.M., Basha S.K. and Samad M.A. (2018), "Heat enhancement of heat exchanger using aluminium oxide (Al_2O_3), copper oxide (CuO) nano fluids with different concentrations", *Mater*. *Today Proc*., **5**, 6481-6488. https://doi.org/10.1016/j.matpr.2017.12.261.

Nezhad, E.Z., Qu, X., Musharavati, F., Jaber, F., Appleford, M.R., Bae, S., Uzun, K., Struthers, M., Chowdhury, M.E.H. and Khandakar, A. (2021), "Effects of titanium and carbon nanotubes on nano/micromechanical properties of HA/TNT/CNT nanocomposites", *Appl*. *Surf*. *Sci*., **538**, 148123. https://doi.org/10.1016/j.apsusc.2020.148123.

Nguyen, M.S.T., Thai, D.K. and Kim, SE. (2020), "Predicting the axial compressive capacity of circular concrete filled steel tube columns using an artificial neural network", *Steel*. *Compos*. *Struct*., **35**(3), 415-437. https://doi.org/10.12989/scs.2020.35.3.415.

Okonkwo, E.C., Wole-Osho, I., Kavaz, D., Abid, M. and Al-Ansari, T. (2020), "Thermodynamic evaluation and optimization of a flat plate collector operating with alumina and iron mono and hybrid nanofluids", *Sustain*. *Energ*. *Technol*. *Assess*, **37**, 100636. https://doi.org/10.1016/j.seta.2020.100636.

Pandit, S. and Sharma, S. (2020), "Wavelet strategy for flow and heat transfer in CNT-water based fluid with asymmetric variable rectangular porous channel", *Eng*. *Comput*. *Germany*., 1-11. https://doi.org/10.1007/s00366-020-01139-z.

Pare, A. and Ghosh, S.K. (2019), "Rheological analyses of aluminum oxide based water nanofluid", *Proceedingd of the International Conference on Thermal Engineering*, Gandhinagar, India, February.

Pastoriza-Gallego, M.J., Casanova, C., Páramo, R., Barbés, B., Legido, J.L. and Piñeiro, M.M. (2009), "A study on stability and thermophysical properties (density and viscosity) of Al_2O_3 in water nanofluid", *J*. *Appl*. *Phys*., **106**, 64301. https://doi.org/10.1063/1.3187732.

Podder, K.K., Chowdhury, M.E., Tahir, A.M., Mahbub, Z.B., Khandakar, A., Hossain, M.S. and Kadir, M.A. (2022), "Bangla sign language (bdsl) alphabets and numerals classification using a deep learning model", *Sensors-Basel*., **22**(2), 574. https://doi.org/10.3390/s22020574.

Saadatmorad, M., Jafari-Talookolaei, R.A., Pashaei, M.H. and Khatir, S. (2021), "Damage detection on rectangular laminated composite plates using wavelet based convolutional neural network technique", *Compos*. *Struct*., **278**, 114656. https://doi.org/10.1016/j.compstruct.2021.114656.

Sadeghi, R., Etemad, S.G., Keshavarzi, E. and Haghshenasfard, M. (2015), "Investigation of alumina nanofluid stability by UV-vis spectrum", *Microfluid Nanofluid*., **18**, 1023-1030. https://doi.org/10.1007/s10404-014-1491-y.

Seaberg, J., Kaabipour, S., Hemmati, S. and Ramsey, J.D. (2020), "A rapid millifluidic synthesis of tunable polymer-protein nanoparticles", *Eur*. *J*. *Pharm*. *Biopharm*., **154**, 127-135. https://doi.org/10.1016/j.ejpb.2020.07.006.

Seguini, M., Khatir, S., Boutchicha, D., Nedjar, D. and Wahab, MA. (2021), "Crack prediction in pipeline using ANN-PSO based on numerical and experimental modal analysis", *Smart Struct*. *Syst*., **27**(3), 507-523. https://doi.org/10.12989/sss.2021.27.3.507.

Sharif, H., Khadimallah, M,A., Naeem, M.N., Hussain, M., Hussain, S. and Tounsi, A. (2021a), "Flow of MHD Powell-Eyring nanofluid: Heat absorption and Cattaneo-Christov heat flux model", *Adv*. *Nano*. *Res*., **10**(3), 221-234. https://doi.org/10.12989/anr.2021.10.3.221.

Sharif, H., Khadimallah, M.A., Naeem, M.N., Hussain, M., Mahmoud, S.R., Al-Basyouni, K.S. and Tounsi, A. (2021b), "The investigation of Magnetohydrodynamic nanofluid flow with Arrhenius energy activation", *Adv*. *Nano Res*., **10**(5), 437-448. https://doi.org/10.12989/anr.2021.10.5.437.

Sheikholeslami, M., Ijaz Khan, M., Chu, Y.M., Kadry, S. and Khan, W.A. (2021), "CVFEM based numerical investigation and mathematical modeling of surface dependent magnetized copper-oxide nanofluid flow using new model of porous space", *Numer*. *Meth*. *Part D E*., **37**(2), 1481-1494. https://doi.org/10.1002/num.22592.

Song, D., Wang, Y., Jing, D. and Geng, J. (2016), "Investigation and prediction of optical properties of alumina nanofluids with different aggregation properties", *Int. J. Heat Mass Transf*., **96**, 430-437. https://doi.org/10.1016/j.ijheatmasstransfer.2016.01.049.

Syarif, D.G. and Prajitno, D.H. (2015), "Synthesis and characterization of Al_2O_3 nanoparticles and water-Al_2O_3 nanofluids for nuclear reactor Coolant", *Adv*. *Mat*. *Res*., **1123**, 270-273. https://doi.org/10.4028/www.scientific.net/AMR.1123.270.

Tran-Ngoc, H., Khatir, S., Ho-Khac, H., De Roeck, G., Bui-Tien, T. and Wahab, M.A. (2021), "Efficient artificial neural networks based on a hybrid metaheuristic optimization algorithm for damage detection in laminated composite structures", *Compos*. *Struct*., **262**, 113339. https://doi.org/10.1016/j.compstruct.2020.113339.

Vaferi, B., Eslamloueyan, R. and Ghaffarian, N. (2016), "Hydrocarbon reservoir model detection from pressure transient data using coupled artificial neural network-Wavelet transform approach", *Appl*. *Soft*. *Comput*. *J*., **47**, 63-75. https://doi.org/10.1016/j.asoc.2016.05.052.

Vakilinejad, A., Aroon, M.A., Al-Abri, M., Bahmanyar, H., Al-Ghafri, B., Myint, M.T.Z. and Vakili-Nezhaad, G.R. (2021),

"Experimental investigation and modeling of the viscosity of some water-based nanofluids", *Chem. Eng. Commun.*, **208**, 1054-1068. https://doi.org/10.1080/00986445.2020.1727451.

Wang, J., Ayari, M.A., Khandakar, A., Chowdhury, M.E., Uz Zaman, S.M., Rahman, T. and Vaferi, B. (2022), "Estimating the relative crystallinity of biodegradable polylactic acid and polyglycolide polymer composites by machine learning methodologies", *Polymers-Basel.*, **14**(3), 527. https://doi.org/10.3390/polym14030527.

Wang, R.T. and Wang, J.C. (2017), "Intelligent dimensional and thermal performance analysis of Al_2O_3 nanofluid", *Energ. Convers. Manag.*, **138**, 686-697. https://doi.org/10.1016/j.enconman.2017.02.010.

Wang, X. and Zhu, D. (2009), "Investigation of pH and SDBS on enhancement of thermal conductivity in nanofluids", *Chem. Phys. Lett.*, **470**, 107-111. https://doi.org/10.1016/j.cplett.2009.01.035.

Wang, X.J., Li, H., Li, X.F., Zhou-Fei, W. and Fang, L. (2011), "Stability of TiO_2 and Al_2O_3 nanofluids", *Chinese Phys. Lett.*, **28**, 86601. https://doi.org/10.1088/0256-307X/28/8/086601.

Wang, X.J., Li, X.F., Wang, N., Wen, X.Y. and Long, Q. (2008), "Influence of SDBS on stability of Al_2O_3 nano-Suspensions", *Proceedings of the Nanophotonics, Nanostructure, and Nanometrology II, International Society for Optics and Photonics*, Beijing, China, January.

Wen, T., Lu, L. and Zhong, H. (2018), "Investigation on the dehumidification performance of LiCl/H_2O-MWNTs nanofluid in a falling film dehumidifier", *Build. Environ.*, **139**, 8-16. https://doi.org/10.1016/j.buildenv.2018.05.010.

Yang, L., Du, K., Niu, X., Li, Y. and Zhang, Y. (2011), "An experimental and theoretical study of the influence of surfactant on the preparation and stability of ammonia-water nanofluids", *Int. J. Refrig.*, **34**, 1741-1748. https://doi.org/10.1016/j.ijrefrig.2011.06.007.

Yan, M., Yousef, Z., Morteza, G., Oslub, K., Khadimallah, MA. and Issakhov, A. (2021), "Computer simulation for stability performance of sandwich annular system via adaptive tuned deep learning neural network optimization", *Adv. Nano Res.*, **11**(1), 83-99. http://doi.org/10.12989/anr.2021.11.1.083.

Yaylacı, E.U., Yaylacı, M., Ölmez, H. and Birinci, A. (2020), "Artificial neural network calculations for a receding contact problem", *Comput Concrete.*, **25**(6), 551-563. https://doi.org/10.12989/cac.2020.25.6.551.

Yousefi, A., Amidi, Y., Nazari, B., and Eden, U.T. (2020), "Assessing goodness-of-fit in marked point process models of neural population coding via time and rate rescaling", *Beilstein J. Nanotech.*, **32**(11), 2145-2186. https://doi.org/10.1162/neco_a_01321.

Zareei, M., Yoozbashizadeh, H. and Hosseini, H.R.M. (2019), "Investigating the effects of pH, surfactant and ionic strength on the stability of alumina/water nanofluids using DLVO theory", *J. Therm. Anal. Calorim.*, **135**, 1185-1196. https://doi.org/10.1007/s10973-018-7620-1.

Zeng, Y., Zhu, X., Xie, J. and Chen, L. (2021), "Ionic liquid coated magnetic core/shell $CoFe_2O_4$@SiO_2 nanoparticles for the separation/analysis of trace gold in water sample", *Adv. Nano Res.*, **10**(3), 295-312. https://doi.org/10.12989/anr.2021.10.3.295.

Zenzen, R., Khatir, S., Belaidi, I., Le Thanh, C. and Wahab, M.A. (2020), "A modified transmissibility indicator and artificial neural network for damage identification and quantification in laminated composite structures", *Compos. Struct.*, **248**, 112497. https://doi.org/10.1016/j.compstruct.2020.112497.

Zhao, W., Li, J., Liu, Z. and Guan, Y. (2009), "Thermal conductivities and viscosities of Al_2O_3-water nanofluids with low volume concentrations", *Proceedings of the International Conference on Micro/Nanoscale Heat Transfer*, Shanghai, China, December.

Zhao, W.L., Zhu, B.J., Li, J.K., Guan, Y.X. and Li, D.D. (2011), "Suspension stability and thermal conductivity of oxide based nanofluids with low volume concentration", *Adv. Mat. Res.*, **160-162**, 802-808. https://doi.org/10.4028/www.scientific.net/AMR.160-162.802.

Zhou, Z., Davoudi, E. and Vaferi. B. (2021), "Monitoring the effect of surface functionalization on the CO_2 capture by graphene oxide/methyl diethanolamine nanofluids", *J. Environ. Chem. Eng.*, **9**(5) 106202. https://doi.org/10.1016/j.jece.2021.106202.

Zhu, B.J., Zhao, W.L., Li, J.K., Guan, Y.X. and Li, D.D. (2011), "Thermophysical properties of Al_2O_3-water nanofluids", *Mat. Sci. Forum.*, **688**, 266-271. https://doi.org/10.4028/www.scientific.net/MSF.688.266.

Zhu, D., Li, X., Wang, N., Wang, X., Gao, J. and Li, H. (2009), "Dispersion behavior and thermal conductivity characteristics of Al_2O_3-H_2O nanofluids", *Curr. Appl. Phys.*, **9**, 131-139. https://doi.org/10.1016/j.cap.2007.12.008.

Zhu, D., Wang, X. and Li, X. (2008), "Influence of SDBS on dispersive stability of Al_2O_3 nano-suspenions", *Proceedings of the International Conference on Micro/Nanoscale Heat Transfer*, Tainan, Taiwan, June.

CC

Appendix. Multilayer perceptron neural networks

Artificial neuron is the smallest meaningfull part in the structure of all artificial neural network types. The artificial neurons are responsible to perform a combination of linear (LPart) and non-linear (NLPart) mathematical operations as follows:

$$LPart = \vec{w}\vec{\varepsilon} + b \quad \text{(A1)}$$

$$NLPart = \psi(\vec{w}\vec{\varepsilon} + b) \quad \text{(A2)}$$

b, w, and ψ are bias and weight coefficients, and transfer function, respectively. Artificial neural networks as their names show are constructed by placing several artificial neurons (ANN) in some successive layers. Indeed, the ANN model is nothing than some weights, biases, and transfer functions. An optimization algorithm adjusts the weight and bias values of the ANN model during the training stage.

The multilayer perceptron neural network is often bulit with two neuronic hidden and output layers. Since the independent variables constitute an input layer, it has no processing neurons. The number of hidden neurons is often found by trial-and-error scenario, while the number of output neurons equal to the number of dependent variables or available classes to be estimated.